

# Hadronization and Charm-Hadron Ratios in Heavy-Ion Collisions

Min He<sup>1</sup> and Ralf Rapp<sup>2</sup>

<sup>1</sup>*Department of Applied Physics, Nanjing University of Science and Technology, Nanjing 210094, China and*

<sup>2</sup>*Cyclotron Institute and Department of Physics and Astronomy,  
Texas A&M University, College Station, Texas 77843-3366, U.S.A.*

(Dated: February 4, 2020)

Understanding the hadronization of the quark-gluon plasma (QGP) remains a challenging problem in the study of strong-interaction matter as produced in ultrarelativistic heavy-ion collisions (URHICs). The large mass of heavy quarks renders them excellent tracers of the color neutralization process of the QGP when they convert into various heavy-flavor (HF) hadrons. We develop a 4-momentum conserving recombination model for HF mesons and baryons that recovers the thermal and chemical equilibrium limits and accounts for space-momentum correlations (SMCs) of heavy quarks with partons of the hydrodynamically expanding QGP, thereby resolving a long-standing problem in quark coalescence models. The SMCs enhance the recombination of fast-moving heavy quarks with high-flow thermal quarks in the outer regions of the fireball. We also improve the hadro-chemistry with “missing” charm-baryon states, previously found to describe the large  $\Lambda_c/D^0$  ratio observed in proton-proton collisions. Both SMCs and hadro-chemistry, as part of our HF hydro-Langevin-recombination model for the strongly coupled QGP, importantly figure in the description of recent data for the  $\Lambda_c/D^0$  ratio and  $D$ -meson elliptic flow in URHICs.

PACS numbers: 25.75.-q 25.75.Dw 25.75.Nq

*Introduction.*— Ultra-relativistic heavy-ion collisions (URHICs) at RHIC and the LHC have created a novel state of strong-interaction matter composed of deconfined quarks and gluons, the Quark-Gluon Plasma (QGP) [1, 2]. The QGP behaves like a near-perfect fluid with small specific shear viscosity, as revealed by the collective flow patterns in final-state hadron spectra being consistent with relativistic hydrodynamic simulations [3–5]. A closely related discovery is the surprisingly large collective flow observed for heavy-flavor (HF) particles and requiring a small diffusion coefficient,  $\mathcal{D}_s$  [6, 7], corroborating the strongly-coupled nature of the QGP. Another interesting finding is an enhancement of baryon-to-meson ratios ( $p/\pi$  and  $\Lambda/K$ ), relative to  $pp$  collisions, at intermediate transverse momenta,  $p_T \simeq 3\text{--}4\text{ GeV}$ , together with the so-called constituent-quark number scaling (CQNS) of the elliptic flow,  $v_2$ , of baryons and mesons. These observations have been attributed to quark coalescence as a hadronization mechanism of kinetic (non-thermalized) partons with thermal partons in the QGP [8–11]. In this paper we will argue that the diffusion and hadronization of HF particles provide a unique opportunity to put these phenomena on a common ground.

The diffusion of low-momentum HF particles has long been recognized as an excellent gauge of their interaction strength with the medium, most notably through their  $v_2$  acquired in non-central URHICs via a drag from the collectively expanding fireball, *cf.* Ref. [7] for a recent review. The large heavy-quark (HQ) mass,  $m_Q \gg T_H$  (with  $T_H \simeq 160\text{ MeV}$  the typical hadronization temperature [12]), also opens a direct window on hadroniza-

tion processes. Thus, HF spectra simultaneously encompass the strong-coupling of the QGP and its hadronization. In particular, the chemistry of the produced HF hadrons [13–17], has recently drawn a lot of attention through the observed enhancements in the  $D_s/D^0$  and  $\Lambda_c/D^0$  ratios at RHIC [18, 19] and the LHC [20, 21]. Reliable interpretations of these data require hadronization models that satisfy both kinetic and chemical equilibrium in the limit of thermal quark distributions as an input. This is also a pre-requisite for an ultimate precision extraction of the HF transport coefficients, reinforcing the intimate relation between HQ diffusion and hadronization. In the kinetic sector, this has been achieved in the resonance recombination model (RRM) [22], where a conversion of equilibrium quark- to  $D$ -meson spectra in URHICs, including their  $v_2$ , has been established on a hydrodynamic hypersurface [23]. As the RRM is based on resonance correlations that develop near  $T_H$  in heavy-light  $T$ -matrix interactions [24], it directly connects to a small HQ diffusion coefficient in the QGP.

In this work, we develop and implement several concepts in quark recombination that will be critical in a comprehensive set-up for HF phenomenology in URHICs. First, we derive a 4-momentum conserving three-body recombination formula for the hadronization into baryons, and verify its quark-to-baryon equilibrium mapping. Second, we devise an event-by-event implementation for HQ distributions obtained from Langevin simulations, which maintains HQ number conservation and satisfies the equilibrium limit of the HF hadro-chemistry. The event-by-event HQ number conservation is pivotal in a precise treatment of space-momentum correlations (SMCs) of in-

dividually transported heavy quarks with anti-/quarks of the underlying hydro background. Both hadro-chemistry and quark SMCs have been challenging issues for instantaneous coalescence models (ICMs) [25, 26]; as such our developments are pertinent well beyond the HF sector. Third, the equilibrium limit of the HF hadro-chemistry is improved by employing a large set of “missing” HF baryon states not listed by the particle data group (PDG), but predicted by the relativistic-quark model (RQM) [27] and consistent with lattice-QCD (lQCD) computations [28, 29]. In Ref. [30] they were shown to account for the large  $\Lambda_c/D^0$  ratio measured in  $pp$  collisions at the LHC (while the environment in  $e^+e^-$  collisions is less conducive to charm-baryon formation).

*Baryons in RRM.*— We first recall the main features of the 2-body RRM [22]. Starting from the Boltzmann equation, resonant quark-antiquark scattering into mesons near equilibrium,  $q + \bar{q} \leftrightarrow M$ , can be utilized to equate gain and loss terms and arrive at a meson phase space distribution (PSD) of the form

$$f_M(\vec{x}, \vec{p}) = \frac{\gamma_M(p)}{\Gamma_M} \int \frac{d^3\vec{p}_1 d^3\vec{p}_2}{(2\pi)^3} f_q(\vec{x}, \vec{p}_1) f_{\bar{q}}(\vec{x}, \vec{p}_2) \times \sigma_M(s) v_{\text{rel}}(\vec{p}_1, \vec{p}_2) \delta^3(\vec{p} - \vec{p}_1 - \vec{p}_2), \quad (1)$$

where  $f_{\bar{q},q}$  are the anti-/quark PSDs,  $v_{\text{rel}}$  their relative velocity,  $\gamma_M(p) = E_M(p)/m_M$ , and  $\Gamma_M$  the meson width. The latter, together with the meson mass  $m_M$  and degeneracy factors, also appear in the resonant  $q + \bar{q} \rightarrow M$  cross section, usually taken of Breit-Wigner type.

The generalization to the 3-body case is conducted in two steps. First, quark-1 and quark-2 recombine into a diquark,  $q_1(\vec{p}_1) + q_2(\vec{p}_2) \rightarrow dq(\vec{p}_{12})$ , whose PSD is obtained in analogy to meson formation, by replacing  $M \rightarrow dq$ ,  $q \rightarrow q_1$  and  $\bar{q} \rightarrow q_2$  in Eq. (1). Diquark configurations are an inevitable component of a thermal QGP approaching hadronization. Second, the diquark recombines with quark-3 into a baryon reusing Eq. (1),

$$f_B(\vec{x}, \vec{p}) = \frac{\gamma_B}{\Gamma_B} \int \frac{d^3\vec{p}_1 d^3\vec{p}_2 d^3\vec{p}_3}{(2\pi)^6} \frac{\gamma_{dq}}{\Gamma_{dq}} f_1(\vec{x}, \vec{p}_1) f_2(\vec{x}, \vec{p}_2) \times f_3(\vec{x}, \vec{p}_3) \sigma_{dq}(s_{12}) v_{\text{rel}}^{12} \sigma_B(s) v_{\text{rel}}^{dq3} \delta^3(\vec{p} - \vec{p}_1 - \vec{p}_2 - \vec{p}_3), \quad (2)$$

where  $s_{12} = (p_1 + p_2)^2$ ,  $s = (p_1 + p_2 + p_3)^2$ ,  $\sigma_B$ : resonance cross section for  $dq + q \rightarrow B$ . This expression depends on the underlying three-quark PSDs on an equal footing.

To check the equilibrium mapping of quark into hadron spectra, we calculate the PSDs for recombination of thermal  $c$  and light quarks ( $q$ ) into  $D^0$  and  $\Lambda_c^+$ , using  $f_{c,q}^{\text{eq}}(\vec{x}, \vec{p}) = g_{c,q} e^{-p \cdot u(x)/T_H}$  with a flow velocity  $u(x)$  on a hydrodynamic hypersurface at  $T_H = 170$  MeV for 0-20% Pb-Pb ( $\sqrt{s_{\text{NN}}} = 5.02$  TeV) collisions (with quark masses  $m_c = 1.5$  GeV,  $m_q = 0.3$  GeV and diquark mass

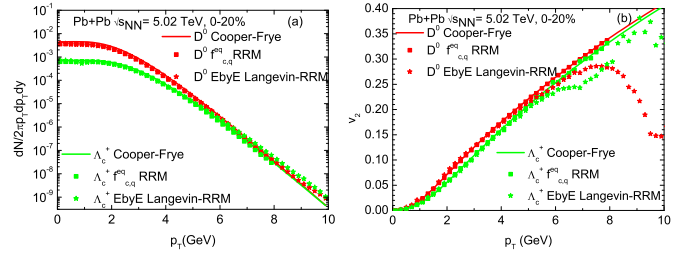


FIG. 1: (Color online) RRM mapping of thermal light- and  $c$ -quark distributions (boxes: thermal, stars: from Langevin simulations with large relaxation rate) into (a)  $p_T$ -spectra and (b)  $v_2$  of  $D^0$  and  $\Lambda_c^+$ , compared to direct  $D^0$  and  $\Lambda_c^+$  hydro results (lines).

$m_{ud} = 0.7$  GeV). The invariant hadron spectra,

$$\frac{dN_{M,B}}{p_T dp_T d\phi_p dy} = \int \frac{p \cdot d\sigma}{(2\pi)^3} f_{M,B}(\vec{x}, \vec{p}) \quad (3)$$

( $d\sigma_\mu$ : hypersurface element), displayed in Fig. 1, confirm that the RRM-generated hadron  $p_T$ -spectra agree with their direct calculation on the same hypersurface in chemical equilibrium, including their elliptic flow  $v_2$ , demonstrated here for the first time for baryons.

*Space-momentum correlations.*— The original derivation of CQNS for light-hadron  $v_2$  within ICMs assumed spatially homogeneous (global) quark distributions in the fireball,  $v_2^q(\vec{x}, \vec{p}) = v_2^q(\vec{p})$  [8, 9]. This is at variance with hydrodynamic flow fields and rendered CQNS to be very fragile upon including SMCs [25]. The application of RRM for mesons [31] could resolve this problem, but no explicit signature of SMCs from recombination processes was identified (see also Ref. [32] using an ICM). Here, we propose that the recent results for the  $\Lambda_c/D^0$  ratio, as well as the  $p_T$  dependence of their  $v_2$ , provide such signatures, and quantitatively elaborate them within our strongly-coupled hydro-Langevin approach [23].

To begin with, we illustrate the pertinent SMCs in Fig. 2 for  $c$ -quark distributions in the transverse plane in different  $p_T$  bins at hadronization. Clearly, low- $p_T$  (0-1 GeV) and higher- $p_T$  (3-4 GeV)  $c$  quarks preferentially populate the inner and outer regions of the fireball, respectively. The spatial density,  $dN/d^3x$ , of Cooper-Frye generated thermal light-quark spectra at midrapidity from the underlying hydro evolution on the same hypersurface shows a similar behavior. As recombination occurs between partons close in both  $\vec{x}$  and  $\vec{p}$  space, the SMCs (not included in studies using ICMs [16, 17]) are expected to be relevant in the formation of charm hadrons especially at intermediate  $p_T$  where signals of the baryon enhancement are prominent.

*Event-by-event Langevin-RRM.*— Since a direct implementation of SMCs with off-equilibrium  $c$ -quark PSDs on the full hadronization hypersurface is not straightforward, we have developed an event-by-event procedure for

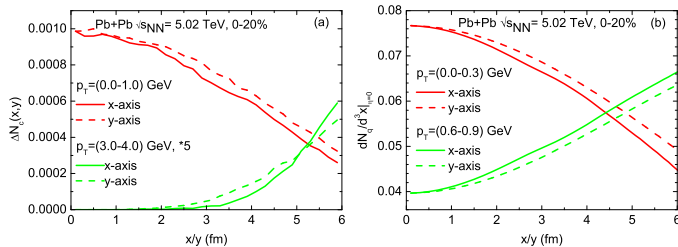


FIG. 2: (Color online) Spatial distributions of (a)  $c$ -quarks from Langevin simulations and (b) light quarks from hydrodynamics in the transverse fireball plane in various  $p_T$  bins.

each diffusing  $c$  quark once it enters a hydro cell at  $T_H$ . Toward this end, we first determine the recombination probability,  $P_{M,B}(p_c^*)$ , for the  $c$ -quark as a function of its momentum in the local restframe (starred variables), convert this into hadron PSDs by sampling the thermal light-quark PSDs at  $T_H$ , and then evaluate the Cooper-Frye formula to compute their  $p_T$  spectra and  $v_2$ , as follows.

Utilizing Eq. (1) for a single  $c$ -quark,  $f_c(\vec{x}^*, \vec{p}_2^*) = (2\pi)^3 \delta^3(\vec{p}_2^* - \vec{p}_c^*) / d^3x^*$  and thermal light antiquarks,  $f_{\bar{q}}(\vec{x}^*, \vec{p}_1^*) = g_{\bar{q}} e^{-E(\vec{p}_1^*)/T_H}$ , in a hydro cell at  $T_H$ , and integrating over the meson momentum,  $\vec{p}^*$ , we obtain

$$P_M(p_c^*) = P_0 \int \frac{d^3\vec{p}_1^*}{(2\pi)^3} g_q e^{-E(\vec{p}_1^*)/T_H} \frac{\gamma_M}{\Gamma_M} \sigma(s) v_{\text{rel}}, \quad (4)$$

representing the recombination probability to form a charm meson  $M$  from a  $c$ -quark of momentum  $\vec{p}_c^*$ . Likewise, one finds for baryon formation

$$P_B(p_c^*) = P_0 \int \frac{d^3\vec{p}_1^* d^3\vec{p}_2^*}{(2\pi)^6} g_1 e^{-E(\vec{p}_1^*)/T_H} g_2 e^{-E(\vec{p}_2^*)/T_H} \times \frac{\gamma_B}{\Gamma_B} \frac{\gamma_{dq}}{\Gamma_{dq}} \sigma(s_{12}) v_{\text{rel}}^{12} \sigma(s_{d3}) v_{\text{rel}}^{dq3}. \quad (5)$$

Here, we have introduced an overall normalization,  $P_0$ , to require the total recombination probability for a  $c$ -quark at rest to be one when summed over all charm-hadron species,  $P_{\text{tot}}(p_c^*=0) = \sum_M P_M(0) + \sum_B P_B(0) = 1$  (with increasing  $p_c^*$ ,  $P_{\text{tot}}(p_c^*)$  drops off and “left-over”  $c$ -quarks will be hadronized via fragmentation [30]). The pertinent PSDs of hadrons from recombination of a single  $c$  quark are then evaluated by sampling the thermal light-quark PSD as  $f_q(\vec{x}^*, \vec{p}_1^*) \sim \sum_n \delta^3(\vec{p}_1^* - \vec{p}_{1n}^*) / d^3x^*$ , with thermal weights in the fluid restframe. Using Lorentz invariance of the meson PSD,  $f_M(\vec{x}, \vec{p}) = f_M(\vec{x}^*, \vec{p}^*)$ , and of  $E_M(\vec{p}^*) \delta^3(\vec{p}^* - \vec{p}_{1n}^* - \vec{p}_c^*) = E_M(\vec{p}) \delta^3(\vec{p} - \vec{p}_{1n} - \vec{p}_c)$ , we plug  $f_M(\vec{x}, \vec{p})$  into Eq. (3) and integrate over  $\vec{p}$  to obtain

$$\frac{dN_M}{dy} \Big|_{y=0} = \sum_n \frac{p \cdot d\sigma_H}{m_M \Gamma_M (d^3x^*)^2} \sigma(s) v_{\text{rel}} \equiv \sum_n \Delta N_M[n], \quad (6)$$

where we have further exploited boost invariance of the underlying hydro evolution to convert the space-time rapidity to momentum space rapidity. For a given  $c$ -quark

and sampling step  $n$ , the meson momentum,  $\vec{p} = \vec{p}_{1n} + \vec{p}_c$ , is fully specified, *i.e.*, the  $\Delta N_M[n]$ 's form a distribution in  $\vec{p}$  whose sum needs to recover the recombination probability,  $P_M(p_c^*)$ , as given above. The  $\Delta N_M[n]$ 's are then binned into  $(p_T, \phi_p)$  histograms to yield the invariant meson spectrum,  $dN_M / p_T dp_T d\phi_p dy$  for a given  $\vec{p}_c$ . An analogous procedure is conducted for charm baryons by sampling two static thermal-light quark PSDs.

Our numerical calculations below are carried out at  $T_H=170$  MeV with resonance widths  $\Gamma_M \simeq 0.1$  GeV,  $\Gamma_{dq} \simeq 0.2$  GeV and  $\Gamma_B \simeq 0.3$  GeV, compatible with the values from the thermodynamic  $T$ -matrix [24], as in our previous work [23]. We have checked that upon doubling all widths, our final results for the  $D$ -meson observables change by less than 10% while the  $\Lambda_c$  suffers additional suppression, by up to  $\sim 30\%$  at intermediate  $p_T \simeq 6$  GeV (not included in our uncertainty estimates shown below). However, for large widths the quasiparticle approximation implicit in the current RRM needs to be replaced by off-shell energy integrals over spectral functions, which will be deferred to a future study. Also note that we utilize a light diquark as “doorway state”, as the heavy-light color-spin interaction is HQ mass suppressed (in either case, the same equilibrium benchmark for the formed baryon applies, irrespective of its substructure). Our charm-hadron spectrum includes all states listed by the PDG plus additional charm baryons as predicted by the RQM and IQCD [30], and essentially figuring in our recent study of 5.02 TeV  $pp$  data for  $\Lambda_c$  production [33]. Based on this spectrum, the probability normalization in Eqs. (4) and (5) amounts to  $P_0=3.6$ . Note that this does not affect the relative abundances of the various hadrons nor their  $p_T$  dependence. The last ingredient needed to obtain the overall norm of the charm-hadron spectra (equivalent to a  $c$  quark fugacity at  $T_H$ ) is the total charm cross section (which again does not affect any ratio or  $p_T$  dependence). With  $d\sigma_{c\bar{c}}/dy \simeq 1.0$  mb from midrapidity ALICE 5.02 TeV  $pp$  data [30], a binary nucleon-nucleon collision number of  $N_{\text{coll}} \simeq 1370$  and a  $\sim 20\%$  shadowing [34] for 0-20%  $\sqrt{s_{\text{NN}}} = 5.02$  TeV Pb-Pb collisions, we obtain  $dN_c/dy \simeq 15.4$ .

*Direct  $\Lambda_c^+ / D^0$  ratio from RRM.* – We now deploy the event-by-event Langevin-RRM simulation with  $T$ -matrix transport coefficients in the QGP [24], first focusing on *direct* production of  $\Lambda_c$  and  $D^0$  (*i.e.*, without feeddown from excited states). The initial  $c$ -quark spectra are taken from the FONLL package [35] as used in our recent study of  $\sqrt{s}=5.02$  TeV  $pp$  data [30]. The resulting RRM-generated spectra of  $D^0$  and  $\Lambda_c^+$  and their ratio right after hadronization are shown in Fig. 3, with and without the inclusion of SMCs (the latter scenario corresponds to our previous implementation [36], where  $c$ -quark conservation was implemented on average, not event by event, *i.e.*, in momentum space only). The SMCs cause the  $D^0$  and  $\Lambda_c^+$  spectra to be significantly harder, and the pertinent  $\Lambda_c^+ / D^0$  ratio is much enhanced at intermedi-

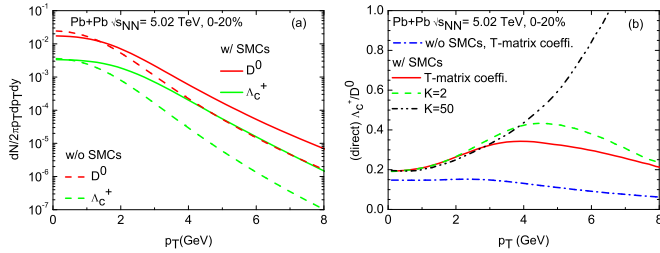


FIG. 3: (Color online) (a): Direct  $D^0$  and  $\Lambda_c^+$  spectra from hydro-Langevin-RRM simulations with baseline  $T$ -matrix  $c$ -quark thermalization rate, in comparison with the counterparts without SMCs. (b): The pertinent  $\Lambda_c^+/D^0$  ratio with and without (dash-dotted line) SMCs, and when using a  $K$ -factor of 2 (dashed line) and 50 (dash-double dotted line) in the baseline  $T$ -matrix rate including SMCs.

ate  $p_T=3-6$  GeV, relative to their counterparts without SMCs. The key mechanism is relatively fast  $c$  quarks moving to the outer parts of the fireball where they find a higher density of significantly harder light-quark spectra for recombination, an effect that enters squared for production of  $\Lambda_c$  baryons. Consequently, their RRM yield toward larger labframe  $p_T$  is further enhanced relative to  $D^0$  mesons.

We have numerically verified that in the limit of large  $c$ -quark thermalization rates, the *absolute*  $p_T$  spectra and  $v_2$  of  $D^0$  and  $\Lambda_c^+$  from the event-by-event Langevin-RRM implementation agree well with the direct hydro calculation (recall Fig. 1), *i.e.*, the “equilibrium mapping” is maintained in the presence of SMCs. Figure 3 also illustrates that, relative to the baseline calculation (solid line), a  $K$ -factor of 2 in the HQ thermalization rate enhances the  $\Lambda_c/D^0$  ratio only a little, much less than the SMC effect.

*Charm-Hadron Spectra and Ratios.* – To enable quantitative comparisons of our event-by-event Langevin-RRM simulations to observables, we include two further ingredients. First, we continue the Langevin simulations for all hadrons through the hadronic phase, starting from their PSDs right after hadronization until kinetic freeze-out of the hydrodynamic evolution at  $T_{\text{kin}}=110$  MeV (as obtained from fits to bulk-hadron  $p_T$  spectra and  $v_2$ ). For  $D$ -mesons we employ our previous thermalization rates [37]; for charm baryons we (conservatively) scale the  $D$ -meson rates with a factor of  $E_D(p^*)/E_{\Lambda_c}(p^*)$  to account for their higher masses; pertinent uncertainties will be illustrated in our plots below. Second, since our approach currently does not include radiative energy loss, we utilize a temperature- and momentum-independent  $K$ -factor of 1.6 in the QGP diffusion rate, chosen to improve the overall description of the LHC and RHIC data.

The spectra of all excited states are used to perform decay simulations [30] to obtain the inclusive spectra of the ground-state  $D^0$ ,  $D^+$ ,  $D_s^+$  and  $\Lambda_c^+$ , which are then

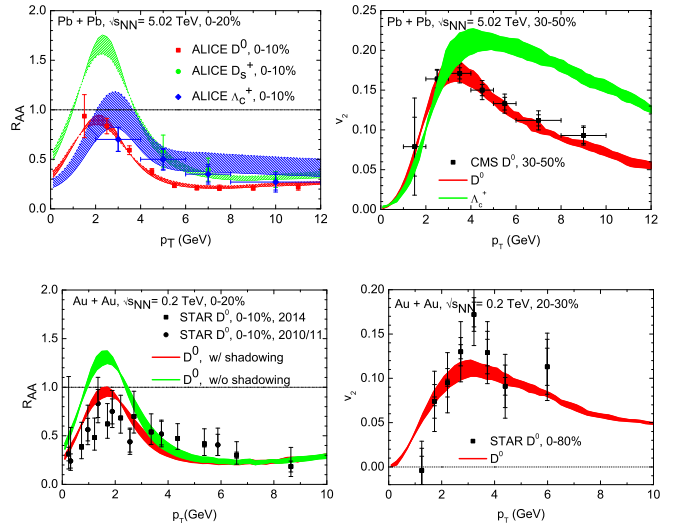


FIG. 4: (Color online)  $R_{AA}$  (left panels) and  $v_2$  (right panels) of  $D^0$ ,  $D_s^+$  and  $\Lambda_c^+$  in Pb-Pb(5.02 TeV) (upper panels) and Au-Au(0.2 TeV) collisions (lower panels), compared to data [20, 21, 38–40]. The uncertainty bands for the  $\Lambda_c^+$   $R_{AA}$  are due to a 50-100% BR for feeddown from excited states above the  $DN$  threshold [30], and for the other observables due to the effects of hadronic diffusion.

converted into nuclear modification factors

$$R_{AA}(p_T) = \frac{dN_{AA}/dp_T}{N_{\text{coll}}dN_{pp}/dp_T}, \quad (7)$$

elliptic flows,  $v_2(p_T)$ , and ratios  $D_s^+/D^0$  and  $\Lambda_c^+/D^0$ . For the  $\Lambda_c$  calculations, the main uncertainty is due to unknown branching ratios (BRs) of excited states, especially those above the  $DN$  threshold which may not decay into a  $\Lambda_c$  final state. As in Ref. [30], we illustrate that by a range of BRs of 50-100% of these states into  $\Lambda_c$  final states (while keeping the denominator of the  $R_{AA}$  fixed using a fit to the  $\Lambda_c$   $pp$  spectrum). Note that their large masses augment the collective flow effect in their contributions to the  $\Lambda_c$  spectra toward higher  $p_T$ . For the  $D$ -meson results, we illustrate uncertainties due to the effects of hadronic diffusion.

A selection of our results is compared to RHIC and LHC data in Figs. 4 and 5. The suppression hierarchy observed in the  $R_{AA}$  data for  $D^0$ ,  $D_s^+$  and  $\Lambda_c^+$  at the LHC is fairly well reproduced, while the  $\Lambda_c/D^0$  ratio tends to be slightly overpredicted. On the other hand, our results tend to underpredict this ratio at RHIC toward lower  $p_T$ . Since the calculated  $\Lambda_c^+/D^0$  ratios approach the chemical equilibrium limit at low  $p_T$ , improved data in this regime at both energies will be very valuable. Another remarkable consequence of the SMCs in the RRM is a much improved description of the  $D$ -meson  $v_2$  data out to higher  $p_T$  compared to our previous results. At RHIC, our results for the  $D^0$ - $R_{AA}$ , without nuclear shadowing, overestimate the low- $p_T$  STAR data [38] significantly. As-

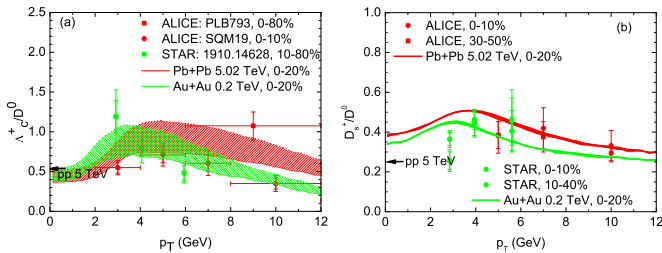


FIG. 5: (Color online) (a):  $\Lambda_c^+/D^0$  and (b):  $D_s^+/D^0$  ratios compared to LHC [20, 21] and RHIC [18, 19] data. The uncertainty bands in the  $\Lambda_c^+/D^0$  ratios are due to a 50-100% BR for  $\Lambda_c$  feeddown from excited states above the  $DN$  threshold [30], and due to hadronic diffusion in the  $D_s^+/D^0$  ratio. The horizontal arrows denote pertinent  $pp$  data.

suming a  $\sim 20\%$  shadowing works better, although most nuclear parton distribution functions do not favor such a scenario. The RHIC results for the  $D^0 v_2$  and the  $\Lambda_c/D^0$  and  $D_s^+/D^0$  ratios are essentially independent of shadowing.

*Summary.* – In the present paper we have advanced the description of HQ hadronization in three critical aspects. First, we developed a 4-momentum conserving recombination model for baryons, which is essential for theoretically controlled calculations. Second, we implemented space-momentum correlations between  $c$ -quarks and the hydro medium on an event-by-event basis. Third, we incorporated an improved charm-hadrochemistry, as previously tested in  $pp$  collisions. We have deployed these developments within our non-perturbative hydro-Langevin-RRM framework, including a moderate  $K$  factor in the QGP diffusion coefficients to simulate hitherto missing contributions from, *e.g.*, radiative interactions. The new components have significant consequences for the interpretation of RHIC and LHC data, and an ultimately improved extraction of HF transport coefficients in QCD matter. Most notably, the SMCs of fast-moving  $c$ -quarks with high-flow partons in the fireball markedly extend the  $p_T$  reach of recombination processes, providing significant enhancements in  $\Lambda_c$  and  $D_s$  production at intermediate  $p_T$ . This also increases the charm-hadron  $v_2$  in this region, in good agreement with RHIC and LHC  $D$ -meson data. Our developments are relevant well beyond the open HF sector in URHICs. We expect the effects of SMCs to shed new light on the large  $v_2$  of  $J/\psi$  [41] and light hadrons at intermediate  $p_T$  where current transport and coalescence models tend to underpredict pertinent data. Even for the “HF puzzle” in pA collisions, where a large  $v_2$  but  $R_{AA} \sim 1$  is observed [7], the SMCs could prove valuable, given the explosive nature of the fireballs conjectured to form in these systems.

*Acknowledgments.* – This work was supported by NSFC grant 11675079 and the U.S. NSF under grant nos. PHY-1614484 and PHY-1913286.

- [1] Y. Akiba *et al.*, arXiv:1502.02730 [nucl-ex].
- [2] E. Shuryak, Rev. Mod. Phys. **89**, 035001 (2017).
- [3] U. Heinz, R. Snellings, Ann. Rev. Nucl. Part. Sci. **63**, 123 (2013).
- [4] C. Gale, S. Jeon, B. Schenke, Int. J. Mod. Phys. A **28**, 1340011 (2013).
- [5] H. Niemi, K. J. Eskola, R. Paatelainen, Phys. Rev. C **93**, 024907 (2016).
- [6] R. Rapp *et al.*, Nucl. Phys. A **979**, 21 (2018).
- [7] X. Dong, Y. J. Lee, R. Rapp, arXiv:1903.07709 [nucl-ex].
- [8] V. Greco, C. M. Ko, P. Levai, Phys. Rev. Lett. **90**, 202302 (2003); Phys. Rev. C **68**, 034904 (2003).
- [9] R. J. Fries, B. Müller, C. Nonaka, S. A. Bass, Phys. Rev. Lett. **90**, 202303 (2003); Phys. Rev. C **68**, 044902 (2003).
- [10] R.C. Hwa, C.B. Yang, Phys. Rev. C **67**, 064902 (2003).
- [11] D. Molnar, S.A. Voloshin, Phys. Rev. Lett. **91**, 092301 (2003).
- [12] A. Andronic, P. Braun-Munzinger, K. Redlich, J. Stachel, Nature **561**, 321 (2018).
- [13] A. Andronic, P. Braun-Munzinger, K. Redlich, J. Stachel, Phys. Lett. B **659**, 149 (2008).
- [14] I. Kuznetsova, J. Rafelski, Eur. Phys. J. C **51**, 113 (2007).
- [15] M. He, R.J. Fries, R. Rapp, Phys. Rev. Lett. **110**, 112301 (2013).
- [16] Y. Oh, C.M. Ko, S.H. Lee, S. Yasui, Phys. Rev. C **79**, 044905 (2009).
- [17] S. Plumari, *et al.*, Eur. Phys. J. C **78**, 348 (2018).
- [18] L. Zhou [STAR Collaboration], Nucl. Phys. A **967**, 620 (2017).
- [19] J. Adam *et al.* [STAR Collaboration], arXiv:1910.14628 [nucl-ex].
- [20] S. Acharya *et al.* [ALICE Collaboration], JHEP **1810**, 174 (2018).
- [21] S. Acharya *et al.* [ALICE Collaboration], Phys. Lett. B **793**, 212 (2019).
- [22] L. Ravagli, R. Rapp, Phys. Lett. B **655**, 126 (2007).
- [23] M.He, R.J.Fries, R.Rapp, Phys. Rev. C **86**, 014903 (2012).
- [24] F. Riek, R. Rapp, Phys. Rev. C **82**, 035201 (2010).
- [25] D. Molnar, arXiv:nucl-th/0408044.
- [26] R.J. Fries, V. Greco, P. Sorensen, Ann. Rev. Nucl. Part. Sci. **58**, 177 (2008).
- [27] D. Ebert, R.N. Faustov, V. O. Galkin, Phys. Rev. D **84**, 014025 (2011).
- [28] A. Bazavov *et al.*, Phys. Lett. B **737**, 210 (2014).
- [29] P. Madanagopalan, R. G. Edwards, N. Mathur and M. J. Peardon, PoS LATTICE **2014**, 084 (2015).
- [30] M. He, R. Rapp, Phys. Lett. B **795**, 117 (2019).
- [31] L. Ravagli, H. van Hees, R. Rapp, Phys. Rev. C **79**, 064902 (2009).
- [32] P.B. Gossiaux, R. Bierkandt and J. Aichelin, Phys. Rev. C **79**, 044906 (2009).
- [33] S. Acharya *et al.* [ALICE Collaboration], JHEP **1804**, 108 (2018).
- [34] K.J. Eskola, H. Paukkunen, C.A. Salgado, JHEP **0904**, 065 (2009).
- [35] M. Cacciari, M. Greco, P. Nason, JHEP **9805**, 007 (1998); JHEP **0103**, 006 (2001).
- [36] M.He, R.J.Fries, R.Rapp, Phys. Lett. B **735**, 445 (2014).
- [37] M.He, R.J.Fries, R.Rapp, Phys. Lett. B **701**, 445 (2011).
- [38] L. Adamczyk *et al.* [STAR Collaboration], Phys. Rev. Lett. **113**, 142301 (2014) [erratum *ibid.* **121**, 229901 (2018)]; Phys. Rev. C **99**, 034908 (2019).

- [39] L. Adamczyk *et al.* [STAR Collaboration], Phys. Rev. Lett. **118**, 212301 (2017).
- [40] A. M. Sirunyan *et al.* [CMS Collaboration], Phys. Rev. Lett. **120**, 202301 (2018).
- [41] S. Acharya *et al.* [ALICE Collaboration], Phys. Rev. Lett. **119**, 242301 (2017).